Transport Modeling and Response Characteristics of Commercial Catalytic Bead Sensors

by

Bethany Christin Brooks

A thesis submitted to the Graduate Faculty of
Auburn University
in partial fulfillment of the
requirements for the Degree of
Master of Science

Auburn, Alabama
May 10, 2015

Keywords: Airline Cabin Environment Research (ACER), Bleed Air Contamination, Methane, Pellistor, Catalytic Bead Sensor, Heat Transfer

Approved by

Ruel A. Overfelt, Chair, Professor of Mechanical Engineering
Bart Prorok, Professor of Mechanical Engineering
Jeffrey Fergus, Professor of Mechanical Engineering

Abstract

Concerns have been raised about contamination events in the bleed air supply of commercial airplanes. Reliable sensors to detect the presence of gases due to the contamination are therefore being considered. Catalytic bead sensors are studied for the detection of combustible gases that may be by-products of bleed air contamination. Two catalytic bead sensors were tested with methane. Steady state and transient experiments were performed to characterize the response of the sensors. A heat transfer model was constructed to better understand the sensors' operation and to be used for considering possible modifications to increase the sensors' sensitivity. The heat transfer coefficient of the sensor system and the operating temperature of the catalytic bead were predicted for use in the heat transfer analysis. Convection was determined to be the dominant method of heat transfer within the catalytic bead system.

Acknowledgements

I would like to express my gratitude to my advisor, Dr. Overfelt, for his patience and guidance throughout my graduate career. I would also like to thank Dr. Prorok and Dr. Fergus for their guidance and for serving on my committee.

I would like to thank my group and class mates who have helped me during this research project. I especially would like to thank Amy Buck, Matthew Roberts, Sadhwi Ravichandran, and Naved Siddiqui for their invaluable assistance and friendship. I would like to extend my gratitude to Mike Crumpler and Steve Moore who were always willing to help me with experiments and to teach me something new. I would to thank my office mates Xingxing Zhang, Eunji Lee, and Fuiling Yang for their friendship during the end of this project.

Finally, I would like to thank my family for their support, encouragement, and patience during this project without whom I would have never been able to experience this opportunity.

This project was partially funded by the U.S. Federal Aviation Administration (FAA) Office of Aerospace Medicine through the National Air Transportation Center of Excellence for Research in the Intermodal Transport Environment (RITE), Cooperative Agreement 10-C-RITE-AU. Although the FAA has sponsored this project, it neither endorses nor rejects the findings of this research.

Table of Contents

List of Tables

List of Figures

Nomenclature

AWG	American Wire Gauge
CH_4	Methane
EDS	Energy Dispersive Spectroscopy
FAA	Federal Aviation Administration
Hz	Hertz
IR	Infrared
LEL	Lower Explosive Limit
MEMS	Micro-Electro-Mechanical System
PPM	Parts Per Million
PSI	Pounds Per Square Inch
SEM	Scanning electron microscope
UEL	Upper Explosive Limit
USB	Universal Serial Bus

Symbols

A_{cs}	Cross-Sectional Area
A_s	Surface Area
C	Concentration
D	Diffusivity
ε	Emissivity
h	Heat Transfer Coefficient
H_c^o	Heat of Combustion
J	Diffusive Flux
k	Thermal Conductivity
$\dot{m}$	Mass Flow Rate
P_{comb}	Power Due to Combustion
P_{cond}	Power Due to Conduction
P_{conv}	Power Due to Convection
P_{rad}	Power Due to Radiation
q_{cond}	Conductive Heat Loss
q_{conv}	Convective Heat Loss
q_{rad}	Radiative Heat Loss
R_1	Resistance of Resistor 1

R_2	Resistance of Resistor 2
R_D	Resistance of Detecting Pelliment
R_R	Resistance of Reference Pelliment
R_T	Resistance of Trim Resistor
σ	Stefan-Boltzmann Constant
τ	Time Constant
T_o	Surrounding Temperature
t_c	Characteristic Diffusion Time
T_s	Surface Temperature
V_{in}	Voltage Supplied
V_{out}	Signal Output
x	Distance

1. **Introduction**

Detection of the presence of harmful gases or the excess of certain gases is vital in many industrial, commercial and consumer applications and specialized gas sensors have been developed for such needs. The necessity to detect combustible gases arises in many industrial applications particularly in mining and other process industries [1]. The most commonly used sensors for combustible gases are catalytic bead sensors. These sensors have been studied and implemented for decades in mines and processing plants, but another possible use involves aircraft cabin environment monitoring.

The environmental control systems of most commercial jet airplanes incorporate an air system that “bleeds” some of the compressed air from the engine to be used within the airplane. As shown in Figure 1, the bleed air system obtains air from the engine at a temperature of 400 °F and a pressure of 30 psi. After passing through an ozone converter and an air conditioning system the air is delivered to the aircraft cabin at a reasonable temperature of 60 °F and a pressure of 11.8 psi. The bleed air is then mixed at a ratio of 50:50 with filtered air recycled from the passenger cabin [2]. Concerns have been raised over the last decade about oils and hydraulic fluids intermittently leaking into engine compressors and contaminating the bleed air supply [2] [3]. These liquids can become degraded, combusted, or pyrolized due to the high bleed air temperatures. The byproducts of these liquids after partial combustion or pyrolysis can include but are not limited to carbon monoxide, carbon dioxide, hydrocarbons, and unburned particulates [3]. Some of these byproducts are believed to cause sickness among passengers and crew [2] [3].

Therefore reliable detection methods for any or all of these liquids and their byproducts has become of increasing interest. This application is the fundamental rationale for the present investigation.

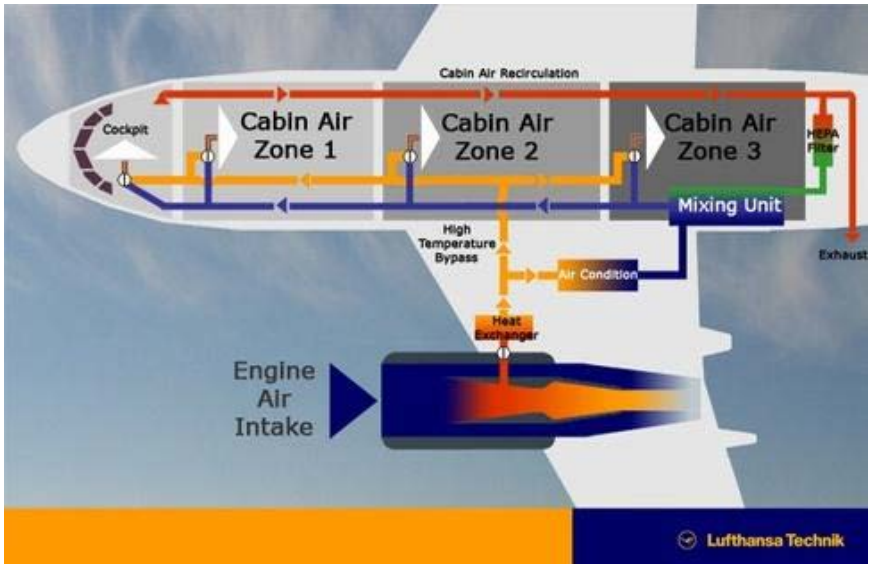

Figure 1: Diagram of aircraft bleed air system **[4]**

Commercial catalytic bead sensors were studied and tested using methane as a calibration gas. Both steady state and transient experiments were performed to analyze the sensors' characteristics. To better understand how the sensors function, a heat transfer model was prepared. From this analysis, the operational mechanisms were quantified and the performance of catalytic bead sensors more fully understood. Accurate modeling can provide insights on possible modifications necessary for catalytic bead sensors to be used in airliner applications.

2. Literature Review

2.1 Pellistors

Although there are numerous methods of detecting combustible gases, the most common sensors used are known in general as pellistors. This name is a portmanteau of the words “pellet” and “resistor” due to the sensing elements being in the form of a pellet and acting as a resistor in an electrical circuit. There are generally two types of pellistors: thermal conductivity sensors and catalytic bead sensors. Catalytic bead sensors operate on the fundamental principle that, in the case of metals, increasing the temperature of the device by inducing combustion of the target gas will increase the resistance. The concentration of the fuel required for an explosive reaction is expressed in terms of whether the fuel is too thin (Lower Explosive Limit, LEL) or too rich (Upper Explosive Limit, UEL). Catalytic bead sensors are used for concentrations near the lower explosive limit of the combustible gas. Conversely, the thermal conductivity sensor does not combust the target gas and therefore is commonly used in applications where concentrations approach the upper explosive limits. In this work the term “pellistor” will be used interchangeably with catalytic bead sensors.

The earliest form of the catalytic bead sensor was simply a coiled filament made of platinum or a platinum group metal. This required that the filament be resistance heated during operation to approximately 900 °C [5]. Unfortunately, the surface of the metal wire would begin to degrade which resulted in long term drift in the resistance. This drift required constant recalibration and meant a short lifespan for the filament. To correct for this, a refractory material

such as alumina was applied to the coiled region of the filament [5]. The detecting pellistor filament (pelliment) in modern devices is covered with a catalyst as seen in Figure 2 to promote combustion at lower temperatures. Using this structural modification, catalytic bead sensors currently on the market operate at temperatures between 300-500 °C [6] [7]. The sensing (detecting) pelliment and reference (compensating) pelliment are each suspended from support posts and placed inside a protective metal housing often referred to simply as a "can." The reference pelliment is not coated with a catalyst and therefor will not promote combustion if operated in this lower temperature regime.

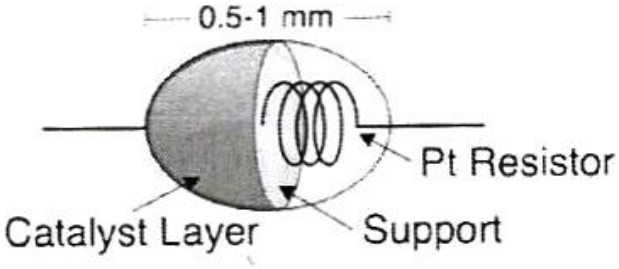

Figure 2: Catalytic bead of pellistor sensor **[1]**

The two pelliments are employed in an electronic circuit known as a Wheatstone bridge. This circuit is commonly used to measure small changes in resistance [8]. Wheatstone bridge circuits consist of four resistors as depicted in Figure 3. The purpose of the reference pelliment is to account for changes in environmental temperature. If the overall environmental temperature changes, the temperature of both pelliments also changes. This causes an increase/decrease in the resistance of both the reference and detecting pelliments which keeps the Wheatstone bridge balanced even for fluctuating environmental temperatures. A supplemental resistor is commonly added to the circuit by the manufacturer to carefully match the operating resistances of both

pelliments which may differ slightly due to manufacturing differences. This is called a trim resistor, and it is placed parallel to the reference pelliment. The signal output of this type of sensor is the voltage across the Wheatstone bridge and should be equal to zero when there is an absence of combustion on the detecting pelliment [5]. The additional resistors used for the bridge (indicated in Figure 3 as R,1 and R,2) do not need to be of any particular resistance value but must match for the detecting pelliment's resistance to be determined from the voltage output.

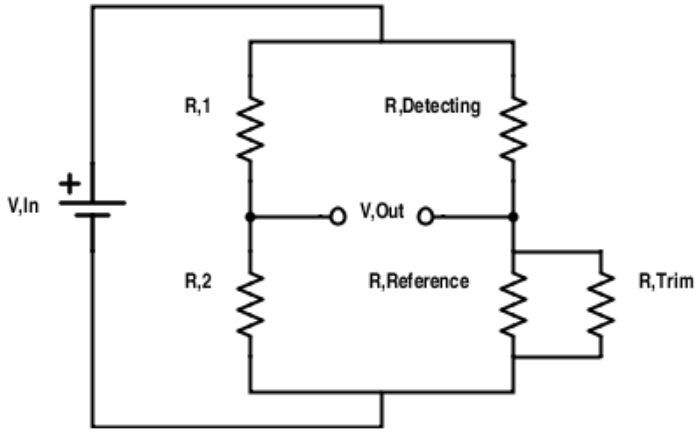

Figure 3: Wheatstone bridge circuit with pelliments and trim resistor

2.2 Combustible Gas Detection

Combustible gases have proved to be an invaluable resource, but they must be used with caution. For combustion to occur the material must be at an appropriate temperature and have a sufficient amount of oxygen. Catalysts can promote combustion at temperatures lower than what is required naturally.

Mining is the most common application where the detection of combustible gases is of critical concern. Throughout the history of mining there have been devastating incidents of pockets of methane seeping out of the earth's crust and building up in mine shafts only to be

ignited [9]. Originally small birds (iconically the canary) were kept in the mine shafts to detect methane buildup. The small birds were later replaced by specially designed lamps which were subsequently replaced by catalytic bead pellistors.

Because these sensors are designed to support combustion, it is necessary to consider what will happen if the concentration of the target gas in the sensor is adequate enough to readily combust and lead to ignition of the entire supply of the combustible gas. This is known as flashback and can be catastrophic. Specialized filters (i.e., flame arrestors) are used between the sensor and the gas supply to avoid such events. Common flame arrestors are constructed of a tight wire mesh or a sintered metal. They hinder the flame's propagation by absorbing some of the heat from the flame front as it passes through the tight channels of the filter causing the flame front temperature to drop below what is required to sustain the flame for that particular fuel.

2.3 Bleed Air Contamination Events in Aircraft

When considering the environment in which passenger jet airplanes operate, one must take into account not only the comfort but also the life support of those on the aircraft. A popular misconception is that most of the air within the cabins of aircraft is recycled meaning that the air is simply filtered and recirculated. In common practice, about half of the air is recycled while the other half comes from outside the aircraft. As detailed below, many commercial jet airplanes contain an environmental control system that "bleeds" some of the pressurized outside air from a compressor stage of a jet engine. In addition to being used for cabin comfort, this air supply is used for wing anti-ice protection and pressurization for various pneumatic systems [2].

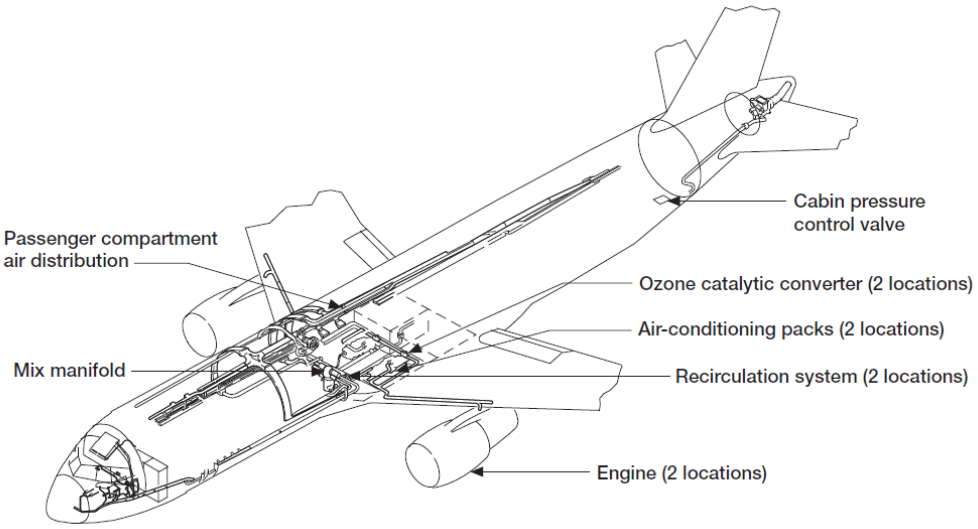

Figure 4: Typical airliner environmental control system **[2]**

An aircraft at typical cruising altitudes is commonly subjected to environmental conditions that are too harsh for humans to survive without aid. The pressure outside the aircraft can be 2.9 psi making the partial pressure of oxygen about 0.5 psi. The outside air temperature is around -70 °F [2]. Outside air is pressurized and heated in the engine compressed and then taken from either of two ports located in the compressor as shown in Figure 5. One of these ports is located at a higher pressure stage of the compressor and the other is at a lower pressure stage. Having these two ports at two different pressures allows the system to obtain air at a usable pressure during all the varying levels of operation of the engines. For example, the high pressure port is used when the engine is at a low power level so that the bleed air is at an acceptable pressure to be used. Conversely, the low pressure port is used when the engine is at a high power level [2].

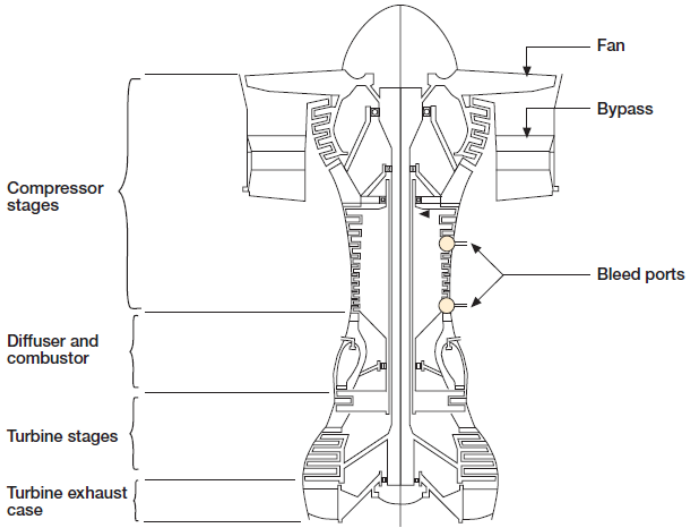

Figure 5: Example jet engine schematic showing common locations for bleed air ports **[2]**

At cruising altitude the bleed air is at a temperature of 400 °F and a pressure of 30 psi. Such high temperatures make the air sterile and free of any living microorganisms. The bleed air is then sent through an ozone converter to reduce the amount of harmful ozone which can be found in the air at such altitudes to an acceptable concentration as set by the Federal Aviation Administration (FAA) [2]. Upon leaving the ozone converter the bleed air is then cooled in the air conditioning packs and the pressure reduced. After the air has been conditioned to a temperature of 60 °F and a pressure of 11.8 psi, the bleed air is mixed at a ratio of about 50:50 with the recycled air from the inside of the aircraft cabin. The air is then supplied to the passenger cabins [2]. As previously stated, concerns have been raised about oils and hydraulic fluids leaking into engine compressors and contaminating the bleed air supply [2] [3] and causing sickness among passengers and crew [2] [3]. There have not been many studies stating the typical concentration of the combustible hydrocarbons (i.e. methane) due to a bleed air

contamination event. One study of three test flights under normal operations found the typical methane concentration to be less than 100ppm [10].

2.4 Transport Phenomena

The processes by which catalytic bead sensors measure a change in concentration of a combustible gas depend upon the principles of heat transfer. As stated previously, these sensors detect the presence of a combustible gas by having a pelliment promote combustion on its surface which raises the temperature of the pelliment which in turn raises the resistance of the platinum wire. The method by which the fuel enters the sensor is gaseous diffusion [7]. The governing relation for this process is known as Fick's First Law. The flux for species diffusion can be approximated as

$$J = D\ \frac{\Delta C}{\Delta x} \tag{1}$$

where J is the diffusive flux(moles/m^2 s), D is the diffusivity of the diffusing species (m^2/s), and $\frac{\Delta C}{\Delta x}$ is the concentration gradient (moles/m^4). The driving force for molecular diffusion is the concentration gradient [11]. Once the rate of combustion at the catalytic bead surface is known the power being released at the catalytic bead surface due to the combusting process can be calculated by accounting for the heat of combustion (ΔH_C^o)(J/mole). This relationship is shown in Equation 2 with $\dot{m}$ being the mass flow rate (moles/s).

$$P_{comb} = (\Delta H_C^o)\dot{m} \tag{2}$$

After the heat is released from the combustion of the fuel, the transfer of that heat must be determined. Some of the heat enters the surface of the catalytic bead changing its temperature and therefore resistance. The heat that is not absorbed is considered to be lost since it does not

contribute to raising the temperature of the catalytic bead. The most common mechanisms by which heat can be transferred are convection, radiation, and conduction as illustrated in Figure 6.

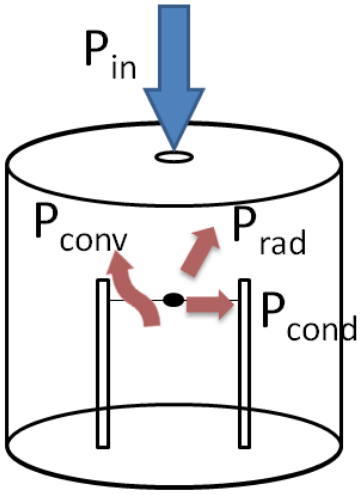

Figure 6: The power into the system due to methane and power losses due to convection, radiation, and conduction

Heat transfer due to convection involves the removal of heat by a fluid. The methods by which it transfers the heat include thermal diffusion and gaseous movement (i.e., advection). The amount of heat lost due to convective cooling is expressed in Equation 3 where h is the interfacial heat transfer coefficient (W/m^2 K), A_s is the surface area (m^2), and ΔT (K) is the difference between the temperature of the combusting gas and the temperature surrounding it [12].

$$q_{conv} = hA_s(\Delta T) \quad 3$$

Heat transfer due to radiation involves the removal of heat by photon emission. Unlike the previously mentioned method of heat transfer, radiation does not require a medium to move the energy. The amount of heat lost due to radiative heat transfer depends upon the temperature

of the surface emitting the photons and the temperature of the environment. It also depends upon the ability of the surface to emit thermal radiation as compared to a black body which can exhibit to maximum emissive capacity. This property of the surface is known as emissivity (ε) and ranges from zero to one. The amount of heat lost due to radiation per unit time can be calculated as shown in Equation 4 where σ is the Stefan–Boltzmann constant (5.67×10^{-8} W/m^2 K^4), A_s is the surface area(m^2), T_s is the temperature of the surface (K), and T_o is the surrounding temperature(K) [13].

$$q_{rad} = \sigma \varepsilon A_s (T_s^4 - T_o^4) \quad (4)$$

Heat transfer due to conduction of a solid involves the removal of heat by atomic vibrations within the lattice structure (i.e. phonons) and the movement of free electrons [14]. The motion of heat is driven by the difference of the temperature of one region of the substance and another. In the case of the catalytic bead sensors, the heat is conducted through the alumina bead to the platinum wire and subsequently away from the catalytic bead down the platinum wire. The amount of heat lost due to conduction per unit time is expressed in Equation 5 where k is the thermal conductivity of the material (W/m^2 K), A_{cs} is the cross-sectional area (m^2), and ΔT (K) is the difference between the temperature of the hottest region and the temperature of the cooler region [13].

$$q_{cond} = k A_{cs} \frac{\Delta T}{L} \quad (5)$$

3. Experimental Procedures

3.1 Commercial Catalytic Bead Sensors

The two models of catalytic bead sensors used for this research differ predominantly in how the pellistor filaments (pelliments) are housed. The VQ10SB model manufactured by SGX (formerly e2v) is constructed of two separate cans each housing a pelliment of which one is the reference pelliment and the other is the detecting pelliment. The cans have an opening to allow the sample gas to diffuse into the housing to reach the pelliments inside. Both the reference and detector are manufactured with flexible leads for connection to the manufacturer provided evaluation board or a user-made circuit board as shown in Figure 7. A trim resistor, matched in the factory with the specific sensor, is used parallel to the reference pelliment.

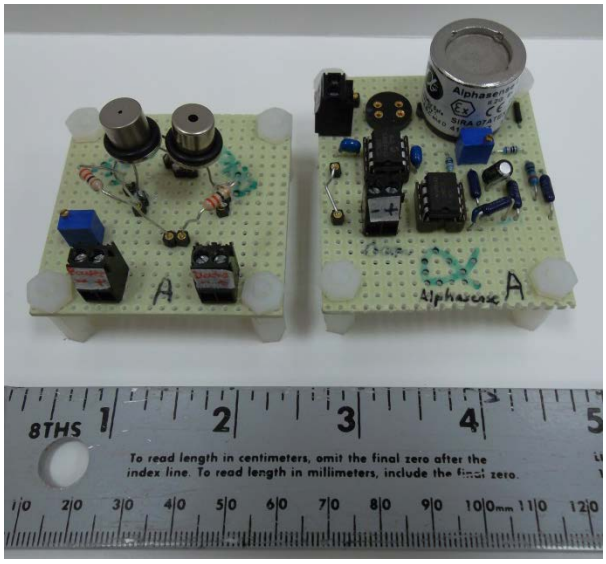

Figure 7: Pellistors studied during this research: SGX VQ10SB on the left and Alphasense CH-A3 on the right

The other catalytic bead sensor studied was the CH-A3 manufactured by Alphasense Ltd. This device incorporates both pelliments into a single housing with a sintered metal flame arrestor. The flame arrestor protects the environment, most commonly in mining applications, from any flames escaping the sensor due to combustible gas concentrations above the lower explosive limit. Although it is a beneficial safety apparatus, the flame arrestor reduces the rate at which the target gas diffuses into the sensor. The sensor is connected to a user-made circuit or commercial instrument by a three pin configuration that is commonly used in the gas sensor industry. Figure 8 shows the internal design of the Alphasense CH-A3 where the pelliments are housed within smaller cans which are then enclosed in a larger single housing.

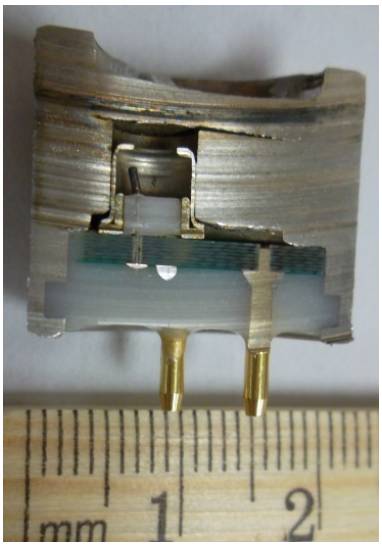

Figure 8: Sectioned Alphasense CH-A3 showing one of the two small interior cans

Table 1: Specifications of pellistors studied. [15] [16]

Model	Power Supply	Manufacturer's Stated Response Time	Design	Manufacturer's Stated Minimum Sensitivity
SGX VQ10SB	2 Volts	(1.25% of 2.5% Concentration) 2 seconds	Reference and detecting pelliments in separate housings	15 mV per% methane
Alphasense CH-A3	3 Volts	(T_{90} from Air to 50%LEL CH_4) <15 seconds (typically <7)	Reference and detecting pelliments in one housing unit	15 to 20 mV per% methane

3.2 Experimental Chamber

The experimental system featured a chamber in which the pure methane gas was mixed with laboratory air resulting in the desired concentration. This ensured that oxygen would be available for the combustion of the methane molecules on the surface of the catalytic bead within the pellistor. This chamber was created by attaching an acrylic tube to a plate allowing one end to be open for the sensors to be inserted and removed as shown in Figure 9. A large test plug was used to seal the chamber. Two fans were mounted to the test plug so that the test gas and the laboratory air would be well mixed. Ports were inserted into the chamber wall for gas inlet, gas outlet, and sensor wire connections. To minimize leaks, moldable clay was used to seal the chamber penetrations.

Figure 9: Experimental chamber used to test target gas concentration

3.3 Data Acquisition

The SGX VQ10SB pellistors were first obtained as a part of a kit provided by the manufacturer that included an evaluation board to mount the pellistors and acquire data. Unfortunately the data provided from the evaluation board is not the raw signal from the Wheatstone bridge needed for detailed analysis. Therefore, a separate circuit was designed and fabricated for use with the VQ10SB pellistors. Conversely, the Alphasense CH4-A3 pellistors were not provided with manufacturers' evaluation boards; a separate circuit board had to be developed before testing could begin. Due to the design differences of the two sensors, the circuits required for each device were slightly different.

Data were acquired using a DATAQ DI-158U module which has positive and negative input terminals and an USB interface for output to a computer. This module and the accompanying software WinDaq was obtained from DATAQ Instruments, Inc. of Akron, Ohio. The data was acquired at rate of 10 Hz per sensor.

3.4 Sensor Experiments

3.4.1 Steady State Testing

Testing for both the SGX and Alphasense pellistors was conducted within the experimental chamber for steady state measurements of varying methane concentrations. Tygon tubing was used to convey the test gas into and ventilated from the experimental chamber. Ball valves were used to ensure that the risk of leaks was minimized throughout the system as seen in Figure 10. A Smart-Trak 2 Series 100 Mass Flow Meter and Controller (Sierra Instruments Inc., Monterey, CA) was used to control the flow rate of test gas into the system Allowing the prescribed flow for an appropriate amount of time resulted in the desired concentration. Data were collected for the baseline through the filling of the chamber and until a final, steady state equilibrium concentration was achieved.

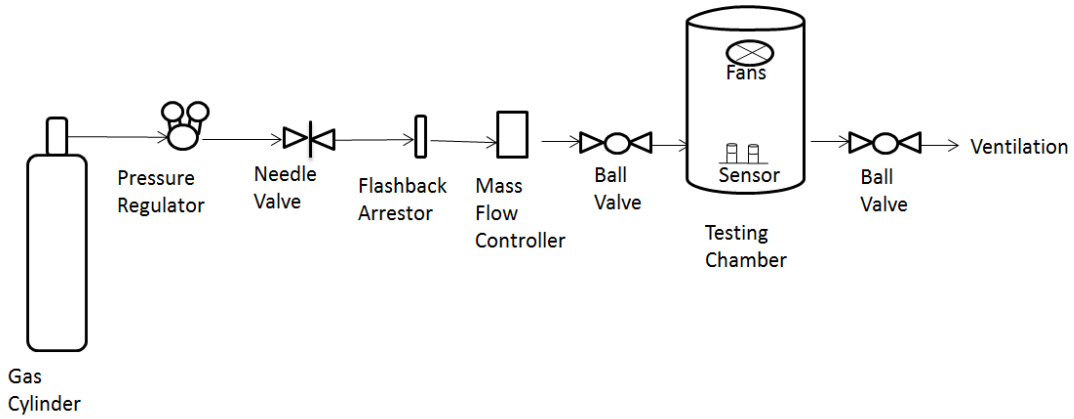

Figure 10: Steady state experimental system

3.4.2 Transient Testing

Transient testing was conducted using the same experimental setup as the steady state testing, but with a few alterations. Instead of the methane gas directly entering the mixing chamber, the gas filled an expandable bladder within the chamber as shown in Figure 9. The bladder was subsequently burst for a near instantaneous mixing of the methane throughout the chamber. This enabled analysis of the sensors' response time to changes in concentration of the target gas.

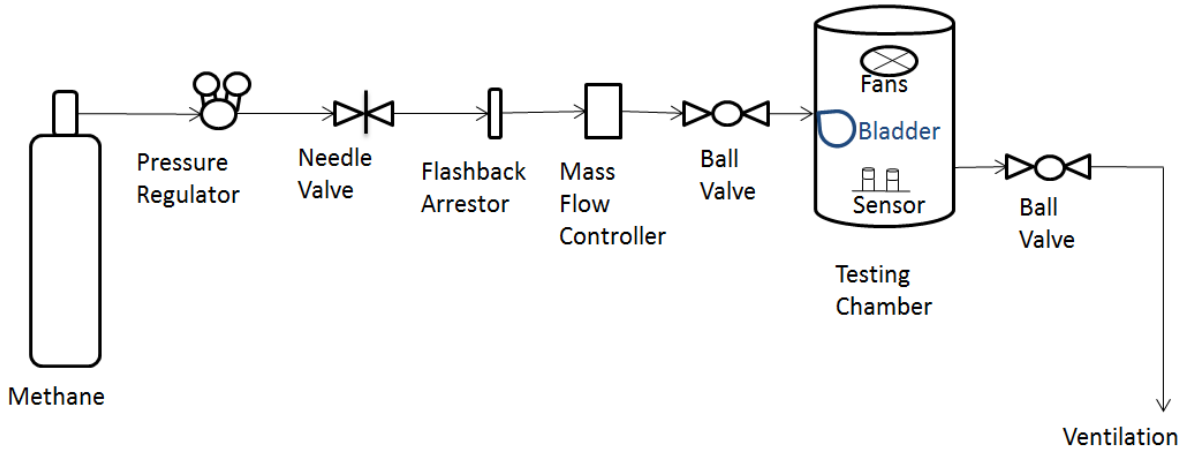

Figure 11: Transient experimental system

3.5 Temperature Determination

3.5.1 IR Camera

Preliminary attempts to measure the temperature of the catalytic bead of the pellistor at target methane concentrations were performed using an infrared camera at steady state gas

concentrations. An IR window was constructed from a germanium disk that was then mounted into the bottom of the gas mixing chamber as described above. The chamber and sensor were then operated horizontally to allow the IR camera to have a direct line-of-sight through the pellistor can openings of the SGX VQ10SB for unobstructed imaging of the catalytic bead. To eliminate potential infrared contamination from the surroundings, a black cloth was used to cover the experimental system.

The infrared camera used to acquire the thermal images was an IR-TCM 640 high resolution IR Camera Module produced by Jenoptik AG of Jena, Germany. Unfortunately the resolution of this thermal imaging technique did not enable precise measurements of changes in bead temperature with increases in methane concentration.

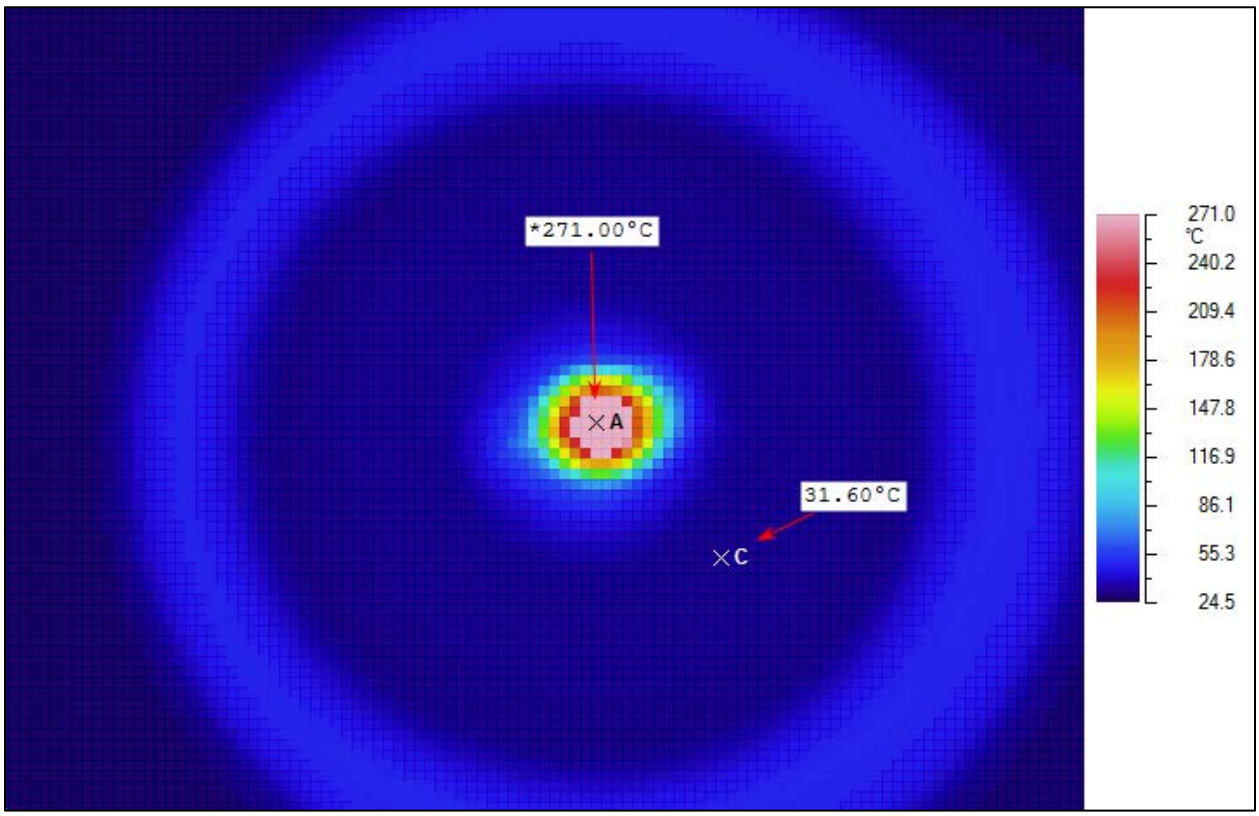

Figure 12: Thermal image of SGX pelliment in can obtained using IR camera.

3.5.2 Temperature Calibration

The changing electrical resistance of the platinum wire filament in a catalytic bead was then exploited to determine the temperature of the bead during exposure to combustible gas.

A Corning hotplate was used to incrementally increase the temperature of an individual SGX pellistor (without the presence of a combustible gas) while simultaneously measuring the resistance across the pelliment. An Agilent 34401A digital multimeter was used to measure the resistance of the pellistor as the temperature was controlled by the hotplate. Filament resistance measurements were recorded using a Visual Basic 6 software program to convey commands to and receive data from the multimeter via RS232 serial interface. An Xplorer GLX handheld device with a PasPort type K temperature sensor (PASCO Scientific, Roseville, CA) was used to acquire the temperature measurements. The resistance and temperature values were obtained at a 0.5 Hz sampling rate. The thermocouple bead was held in intimate contact with the pellistor can and aluminum holder as shown in Figure 13. It was assumed that when the larger thermal mass of the pellistor can reached a steady state temperature, the smaller pelliment also reached the same temperature and was at steady state as well.

The leads of the SGX VQ10SB, that function as support posts for the pelliment, were connected to 12 AWG solid copper wires by folding the ends of the larger diameter copper wires over the ends of the smaller diameter leads of the pellistor and compressed so that the smaller leads were held securely within the fold of the copper wire. This approach was used because the elevated test temperatures were higher than the melting points of conventional solders. The diameter of the solid copper wires was chosen so that their resistance would be negligible to that of the pelliment.

Fiberglass insulation was used to reduce the heat loss due to convection. The temperature range used was considerably below the softening temperature of fiberglass. The pellistor and thermocouple assembly was assembled into a specially designed aluminum fixture that was then placed on the hot plate. The fixture was created out of an unknown aluminum alloy obtained from the mechanical shop. The fixture was designed with a gas inlet and an outlet as well as a gas measurement cavity for the subsequent methane measurements discussed below. Insulation was carefully positioned around the assembly to cover the pellistor can and aluminum fixture. Fiberglass is noncombustible, but due to the potential burning of dyes in the insulation a ventilation hose was used to remove any fumes that were generated.

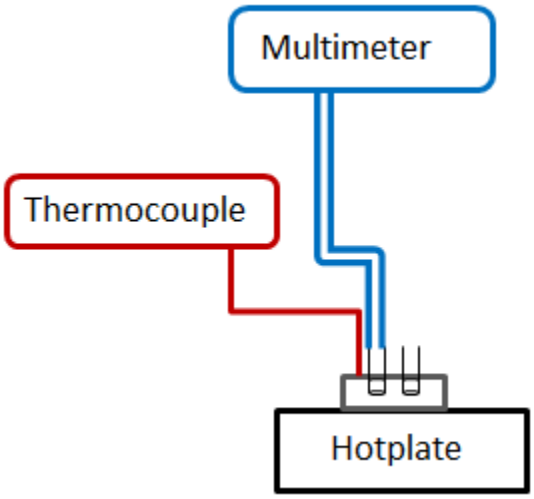

Figure 13: Calibration setup for resistance measurements as a function of temperature

3.5.3 Methane Measurements

The aluminum fixture utilized for temperature calibration measurements was designed to enable test gas to be introduced to the pellistor without changing the experimental set-up. This reduced handling of the components and enhanced repeatability of the measurements.

These methane tests differed from the steady state and transient gas measurement tests previously discussed in that these tests required the target gas to continuously flow over the sensors. Flowing gas was supplied to the sensors by two Smart Trak 2 mass flow controllers (Sierra Instruments Inc., Monterey, CA.). A mass flow controller with a range of 0-500 sccm was used to control the flow of shop/compressed air while a mass flow controller with a range of 0-10 sccm was used for the pure methane. The desired concentrations of methane were obtained by changing the flow rates of the air and methane according to the following equation:

$$desired\ \%\ CH_4 = \frac{flow\ rate\ of\ \ CH_4\ in\ sccm}{flow\ rate\ of\ air\ in\ sccm + flow\ rate\ of\ \ CH_4\ in\ sccm} \times 100\% \qquad 6$$

In each experiment, a baseline condition was established with only air flowing and then methane was added to the flow at the specific flow rate for the desired concentration. Once the pellistor output reached a steady state, the change in signal was determined and the steady state value was selected to represent the appropriate value for the target concentration of methane.

4. Results and Discussion

4.1 Steady State Results

Working sensor calibrations were not provided by the manufacturers for the two models of commercial catalytic bead sensors examined in this work. The results of the steady state experiments were used to establish appropriate calibration curves for the combustible gas methane. As stated previously, these steady state tests were performed in a chamber that allowed the target gas to diffuse into the sensor.

4.1.1 SGX VQ10SB

Methane calibrations for the SGX (company formerly called “e2v”) catalytic bead sensor are specific for each sensor’s pair of pelliments. A calibration for one particular sensor cannot be used for a different sensor of the same model as shown by two different calibration curves in Figure 14.

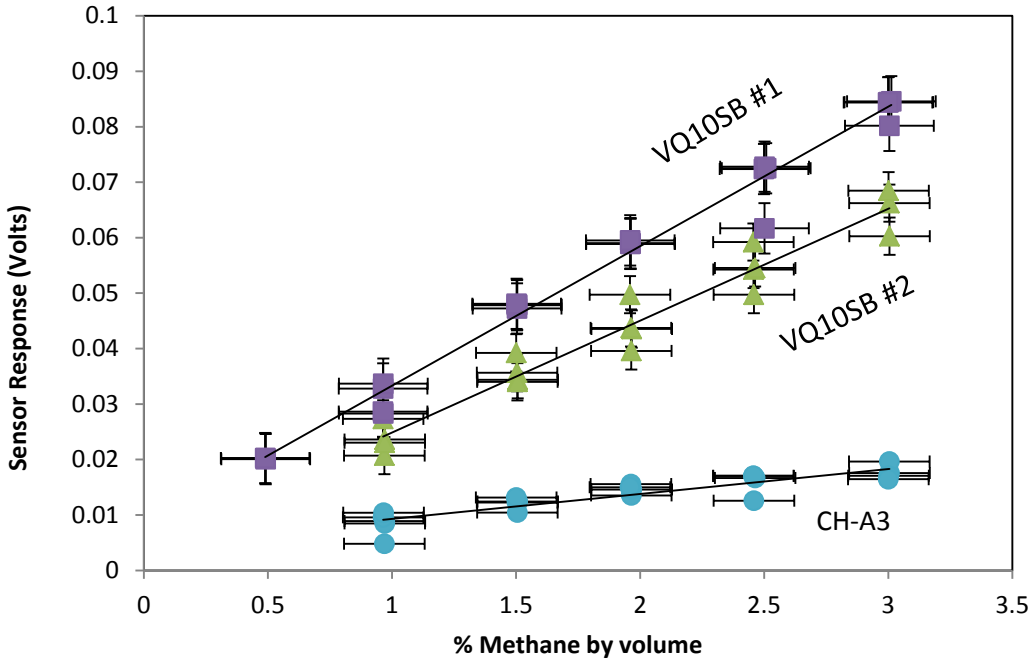

Figure 14: Methane calibrations for two separate SGX VQ10SB sensors (purple squares and green triangles) and one Alphasense CH-A3 (blue circles).

4.1.2 Alphasense CH-A3

As with the SGX model, the Alphasense CH-A3 methane calibrations differed with each specific sensor. The slopes of these calibrations are considered to be the sensor's sensitivity (volts per methane concentration in %). A typical calibration curve for the two sensors studied is presented in Figure 14. The sensitivity of the Alphasense CH-A3 sensors was typically less than the SXG model. According to the manufacturer's specifications listed in Table 1 the sensitivities of both these models should be approximately 15mV per % methane. The decreased sensitivity of the Alphasense CH-A3 is possibly due to premature aging as a result of vigorous testing at near LEL methane concentrations or possibly due to reduced catalytic activity as a result of surface contamination from poisoners or inhibitors.

4.2 Heat Transfer Coefficient Determination

As previously described the transient experiments were performed in the same diffusion chamber as the steady state testing with the only difference being the use of an expandable bladder to introduce an instantaneous amount of target gas to the system. The final steady state results from the transient methane testing were utilized to compare with the previous calibration data. The final steady state results for both of the catalytic bead sensors had similar sensitivities to previous calibrations.

The transient methane experiments were used to determine each sensor's experimental time constant. The time constant of a first order system undergoing change is defined as the time it takes to reach 1-1/e or about 63.2% of its final asymptotic value as seen in Figure 15. As previous research showed, the mixing of the methane and air within the chamber can be considered instantaneous immediately after the bursting of the bladder [17]. The time constant was calculated by applying Equation 7 to the transient experimental data. This was accomplished by using the Curve Fitting Tool of the Matlab software (MathWorks, Inc., Natick, MA). In Equation 7, V_{out} is the sensor signal output (volts), t is time, τ is the time constant, a and c are constants.

$$V_{out} = a\left[\exp\left(-\frac{t}{\tau}\right)\right] + c \qquad 7$$

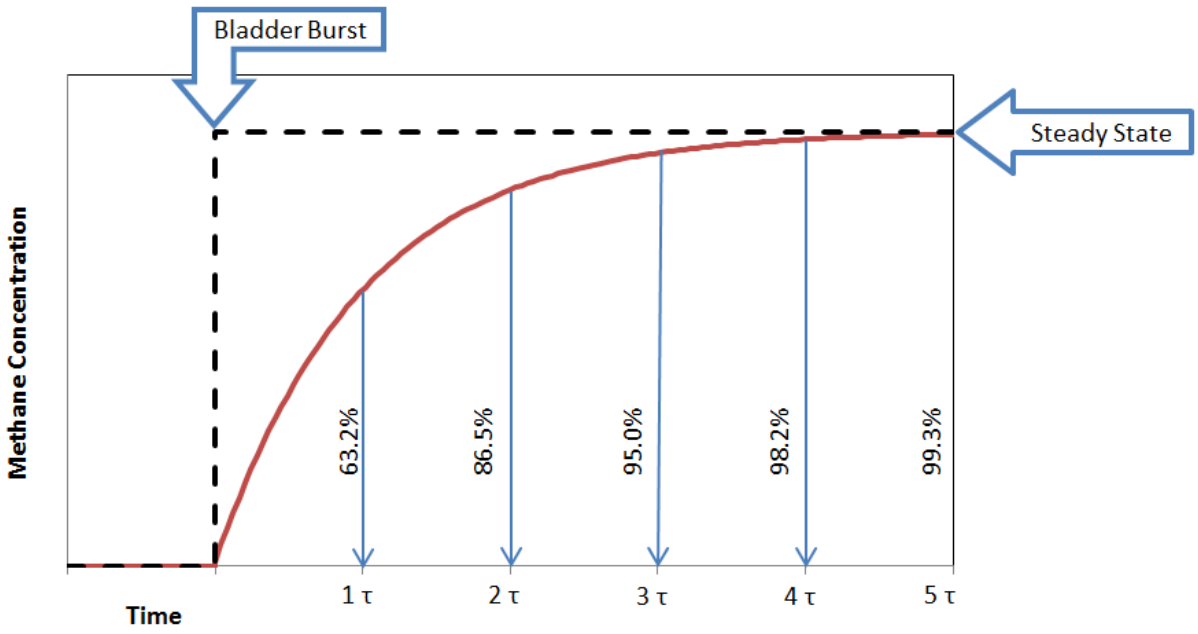

Figure 15: Typical first-order system response curve showing time constant (adapted from **[18]**)

Figure 16 shows typical transient methane experimental results for the SGX catalytic bead sensor. The results of curve fitting such data produced time constant values ranging from 2.0s to 2.7s for the SGX sensor. The average of these time constant values was found to be 2.4s.

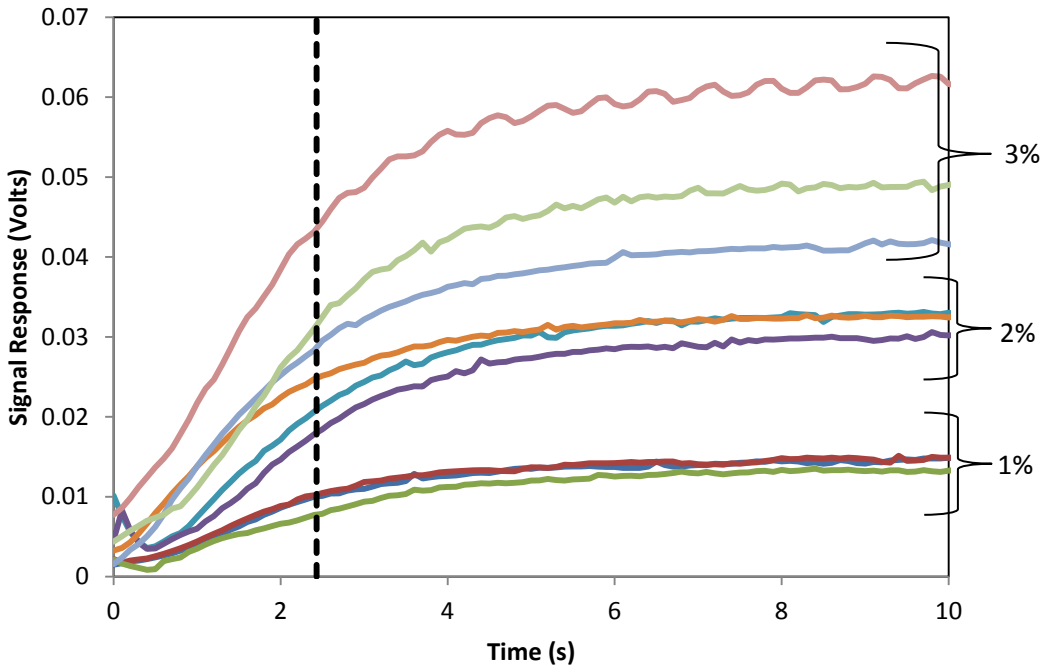

Figure 16: Transient rise in methane concentrations with average time constant (dotted line) for SGX sensor

Using this time constant value the heat transfer coefficient was calculated by the definition of the thermal time constant for convection as shown by Equation 8 where ρ is the density (g/m^3), V is the volume (m^3), C_p is the heat capacity (J/ (g K)), h is the heat transfer coefficient (W/ (m^2 K)), and A_s is the surface area of the bead (m^2). The value for the heat transfer coefficient during heat-up for the SGX sensor was calculated as approximately 77 W/(m^{2}K). This form of the equation takes into account the coiled platinum wire within the bead and the alumina encapsulating it.

$$\tau = \frac{\rho_{coil} V_{coil} C_{p,coil} + \rho_{alumina} V_{alumina} C_{p,alumina}}{h A_s} \quad (8)$$

Table 2: Calculation of Heat Transfer Coefficient

Input Parameters	
Density of Platinum Coil	2.1×10^{6} g/ m^3
Volume of Platinum Coil	3.7×10^{-12} m^3
Specific Heat Capacity of Platinum Coil	0.13 J/(g K)
Density of Alumina	4.0×10^{6} g/ m^3
Volume of Alumina	1.1×10^{-10} m^3
Specific Heat Capacity of Alumina	1.3 J/(g K)
Surface Area	3.1×10^{-6} m^2
Time Constant	2.4 s
Heat Transfer Coefficient	77 W/(m^2K)

To determine if the gaseous diffusive time constant for this process should be considered, the characteristic time for diffusion of methane into the sensor was calculated. An order of magnitude estimate for the diffusion of methane into the gas sensor was calculated by the relationship shown in Equation 9 where t_c is the characteristic time (s), a is the distance through which the methane diffuses (m), and D is the diffusivity of methane in air (1.5×10^{-4} m^2/s) [19].

$$t_c = \frac{a^2}{D} \qquad 9$$

As expected the order of magnitude calculated methane for the characteristic diffusion time is very small, 10^{-4}s, several orders of magnitude less than the characteristic heat-up time experimentally determined for the sensor. It can be concluded, therefore, that the diffusive supply of methane for combustion is not rate limiting for the sensor response time.

4.3 Temperature Determination

In order to thoroughly understand the heat transfer of the system, the temperature of the catalytic bead was investigated during operation in the presence of methane.

4.3.1 Temperature Calibration

The resistance of the platinum filament in the catalytic bead pelliment of a SGX sensor was measured over a range of temperatures imposed by a hot plate without the presence of any combustible gas. The experiment was conducted five times to examine repeatability. Excellent experimental repeatability was obtained by testing one pelliment consecutively 5 times without moving the pelliment. As depicted in Figure 17 the average of the five experiments' linear fits showed that the room temperature resistance of the pelliment is approximately 2 Ohms. The margin of error for this average is approximately ±6% of the resistance. The resistance of the platinum wire, as a function of the increasing temperature, from which the bead is suspended was subtracted from the resistance measurements obtained. This was due to the hotplate technique heating the entire pelliment, whereas normal sensor operation would have the bead being at the increase temperature due to combustion. Unfortunately, the design and construction of the Alphasense CH-A3 catalytic bead sensor contained an internal printed circuit board and thus was not a candidate for similar testing on the hot plate.

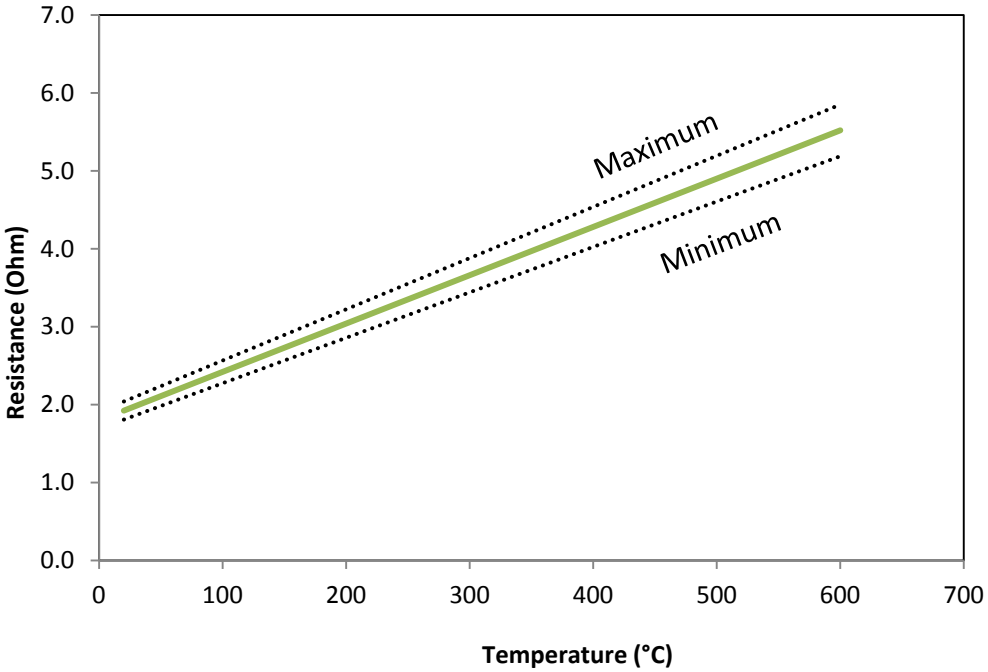

Figure 17: Temperature calibration of SGX detecting pelliment with average of five tests (solid green line) and margins of error (±6% resistance)

4.3.2 Methane Calibration

The same catalytic bead sensor used in the temperature calibration was then subjected to methane exposures. Note that the experimental design enabled the methane exposures to be conducted immediately after the hot plate experiments so that the sensor was not moved between the two types of experiments. The resistance of the detecting pelliment was then calculated from the Wheatstone bridge output of the sensor. This calculation was performed using Equation 10 where V_{out} is the out-of-balance bridge voltage as the signal response (Volts), R_1 and R_2 are the resistances of the resistors used to complete the circuit (Ohms), R_D is the unknown resistance of the detecting pelliment (Ohms), $R_{R,T}$ is the combined resistance of the reference pelliment and trim resistor (Ohms), and V_{in} is the voltage supplied to the circuit (volts). Figure 18 illustrates the resistance of the detecting pelliment in response to the methane exposures.

$$V_{out} = \left[-\frac{R_2}{R_1+R_2} + \frac{R_D}{R_{R,T}+R_D}\right] V_{in} \quad (10)$$

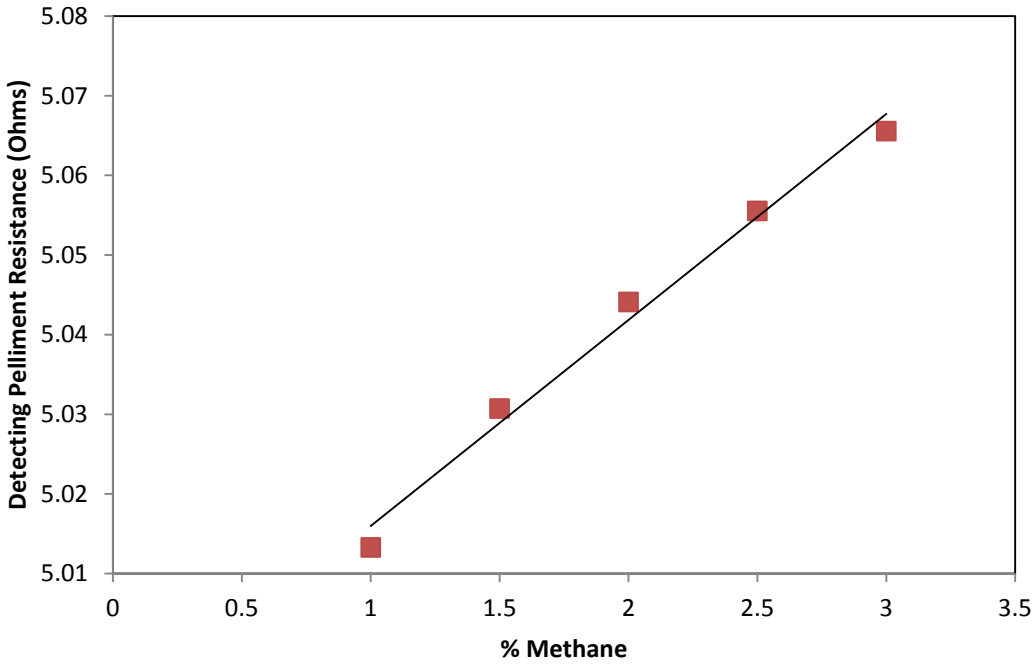

Figure 18: SGX platinum filament resistance versus methane exposure

4.3.3 Temperature Prediction

Once the resistance of the platinum filament in the SGX catalytic bead sensor was quantified with respect to hot plate temperature and then also the methane exposure, the relationship between the catalytic bead surface temperature and methane concentration could be determined. The predicted temperature according to the experimental results described above is shown in Figure 19.The catalytic bead temperature is approximately 518-526 °C depending upon the specific concentration of methane. This assumes that the laboratory environment is about 20°C and 1 atm. As discussed in the Experimental Procedures, the combustion process

temperature was estimated using the infrared camera to be least 270 °C. Note that the poor resolution of the IR camera limited a more precise measurement

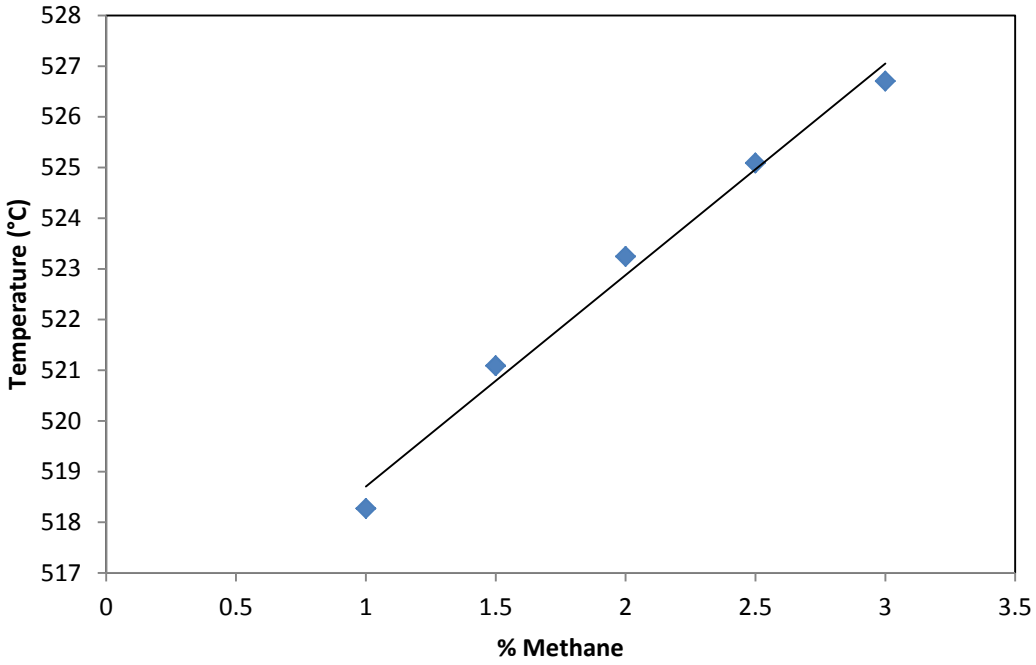

Figure 19: The experimentally determined temperature of the SGX detecting pelliment as a function of methane concentration

4.4 Heat Transfer Model

Measurements of the SGX pelliment wire diameter and bead radius were determined by scanning electron microscopy. As seen in Figure 20 the radius of a typical pelliment bead is 500-600 μm and the diameter of a typical platinum wire filament is 24μm. These measurements will be used in the following heat transfer analysis.

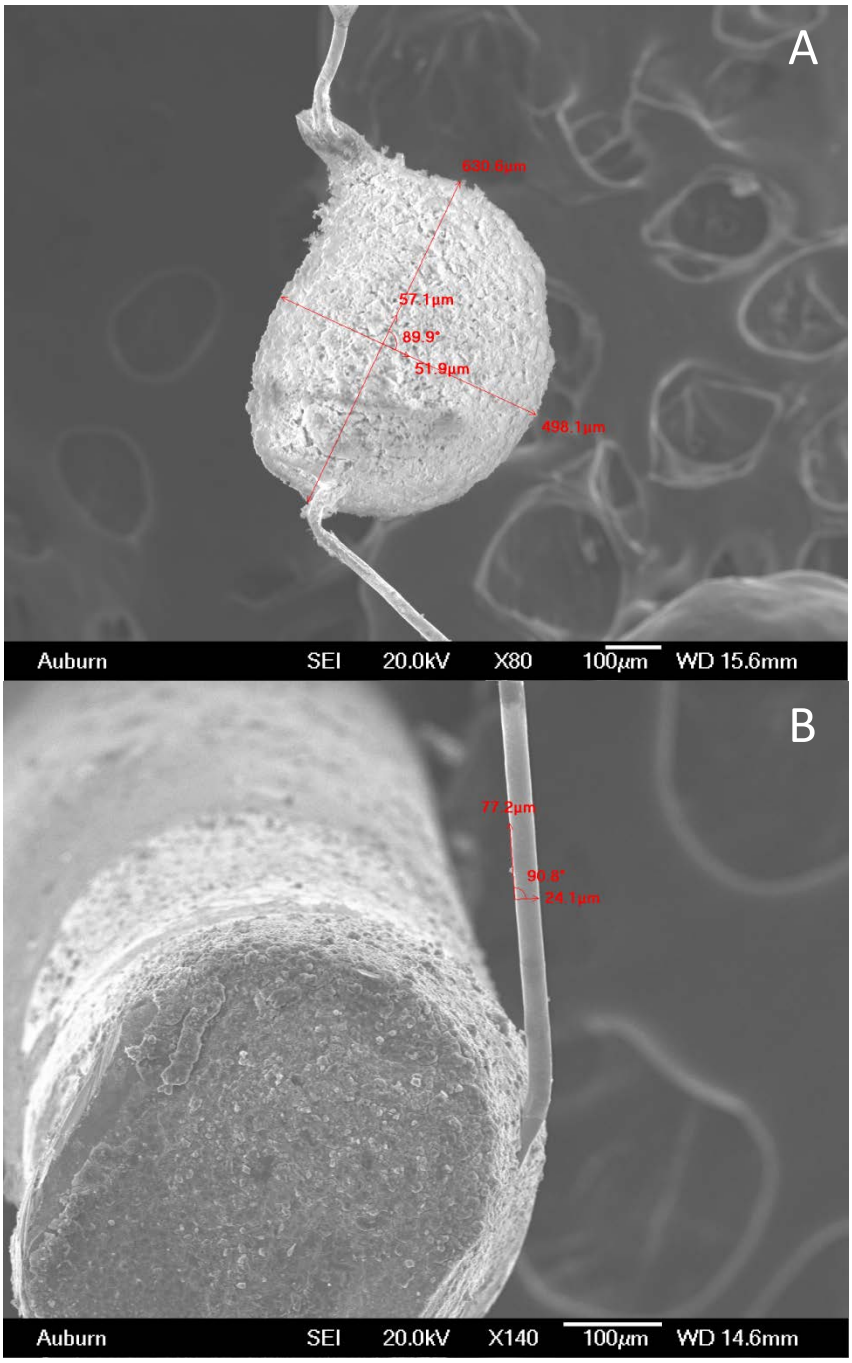

Figure 20: Scanning electron microscope images of alumina bead (A) radius and platinum wire (B) diameter

The maximum power entering the system due to the diffusion and complete combustion of methane was estimated considering the pure diffusion of methane gas in air (Equation 1) followed by the complete combustion of methane (Equation 2). The maximum possible power release at the catalytic bead surface is then given by Equation 11 below. The input parameters for calculation using1% methane by volume is given in Table 2 below. The maximum sustained power for complete combustion of 1% methane diffusing into an SGX sensor was estimated to be approximately 0.13W.

$$P_{comb} = (\Delta H_C^o)\left(A_{cs} D \frac{\Delta C}{\Delta x}\right) \quad 11$$

Table 3: Sample Calculation of Power due to combustion

Input Parameters	
Heat of Combustion	8.02×10^{5} J/mole
Cross Sectional Area	2.7×10^{-6} m^2
Diffusivity [19]	1.5×10^{-4} m^2/s
Change in Methane Concentration	0.75 moles/m^3
Distance	1.9×10^{-3} m
Power Due to Combustion	0.13 W

The catalytic bead sensor will not absorb 100% of the power released by the combustion of methane. Some power will be lost by radiation from the process zone to the surroundings (sensor container), some power will be lost by convection to the surrounding atmosphere and some power will be lost by conduction through the filament lead wires to the surroundings as illustrated in Figure 6. According to the experimental temperature estimates shown in Figure 19, 1% methane will produce a catalytic bead temperature of approximately 518 °C. The following power loss calculations will assume a catalytic bead temperature of 518 °C.

The power loss due to convection, radiation, and conduction were calculated using Equations 3, 4 and 5, respectively. Table 4 lists the various parameters for the calculations and the power loss due to each method of heat transfer. From these values it is seen that the heat lost due to convection is predicted to dominate the heat transfer associated with the catalytic bead. This result is consistent with published research for such devices [9]. It should also be noted that the total power loss calculated for the catalytic bead is 0.078W, in general agreement with the calculation of total combustion power available of 0.13W. Assuming all of the heat generated from the combustion of the gas is absorbed into the bead, about 30% of the power lost is due to convective heat transfer.

Table 4: Sample Calculation of Power Loss

Input Parameters for Radiation	
Stefan-Boltzmann Constant	5.67×10^{-8} W/(m^2 K^4)
Surface Area of Bead	1.1×10^{-6} m^2
Surface Temperature of Bead	791 K
Surroundings Temperature	293 K
Emissivity of Alumina	0.5
Power Loss Due to Radiation	0.012 W
Input Parameters for Conduction of One Side of Wire	
Thermal Conductivity of Wire [20]	72.8 W/(m° C)
Cross Sectional Area of Wire	4.6×10^{-10} m^2
Difference in Temperature	498 °C
Length of Wire	1.4×10^{-3} m
Power Loss Due to Conduction	0.012 W
Input Parameters for Convection	
Heat Transfer Coefficient	77 W/(m^2 K)
Surface Area of Bead	1.1×10^{-6} m^2
Difference in Temperature	498 K
Power Loss Due to Convection	0.042W
Total Power Loss	0.078W

5. Conclusions

The steady state characteristics for the SGX (e2v) VQ10SB and Alphasense CH-A3 were studied using methane. Catalytic bead sensor technology proved to be a reliable and fast gas sensing technology. The sensitivities of both commercial sensors were found to be adequate for typical industrial applications.

Transient testing was performed to calculate the heat transfer coefficient of the SGX VQ10SB sensor system. Using a curve fit of the rise data from the transient tests, the heat transfer coefficient was calculated to be about 77 W/m^2K.

A technique was developed using a hotplate to determine the relationship between the resistance and the temperature of the detecting pelliment. Using this method the operational temperature of an SGX VQ10SB catalytic bead was measured to be between 518-526 °C depending upon the concentration of methane present.

Using the measured catalytic bead temperature and empirical heat transfer coefficient, a working heat transfer model of the SGX VQ10SB catalytic bead sensor was formulated. The heat transferred away from the catalytic bead surface by convection was determined to be the dominant mode of power loss for this sensor system. Improvements to the sensitivity of this sensor technology might be possible by reducing the power loss due to convection heat transfer. Methods to lower the temperature gradients within the sensor system would also help reduce power loss and improve sensitivity as well.

6. Future Work

Further research will determine whether these sensors are sensitive enough for detection of the smaller concentrations expected from a small oil or hydraulic fluid leak during a bleed air contamination event in an aircraft. To increase performance of the sensors, modifications need to be considered. Accounting for convection being the dominant mode of heat transfer within the sensors, possible modifications could include temperature gradient reduction. For example, increasing the temperature of the sensor housing would decrease the temperature difference between the combustion zone and its surroundings. According to the heat transfer model, this would reduce the heat transfer away from the catalytic bead not only due to convection but conduction and radiation as well.

Another direction by which modifications could be approached is the study of how to optimize the gas concentration. One such technique could use a zeolite as a means to “amplify” the gas concentration. This type of material has a property that allows it to absorb a designated type of molecule from the environment and then release it upon heating. Zeolites have been studied for methane storage [21]. This is made possible by the material’s microstructure having micropores or channels that capture the target molecules. Once it has been determined that all the target molecules have been absorbed from the environment of a known volume, the material can be transferred to a smaller volume to release the molecules (methane) for detection with catalytic bead sensors. This would in effect increase the concentration within the smaller volume, but if the original volume was known then the original concentration could be calculated.

More research would also be performed with the micro-electro-mechanical (MEMS) sensor counterpart for the traditional catalytic bead sensors. These new sensors boast lower power consumption and increased ruggedness [9]. Some manufacturers are beginning to produce commercially available MEMS pellistor sensors as shown in Figure 21. Unfortunately, these sensors are stated as having equal sensitivity to the traditional catalytic bead sensors [9].

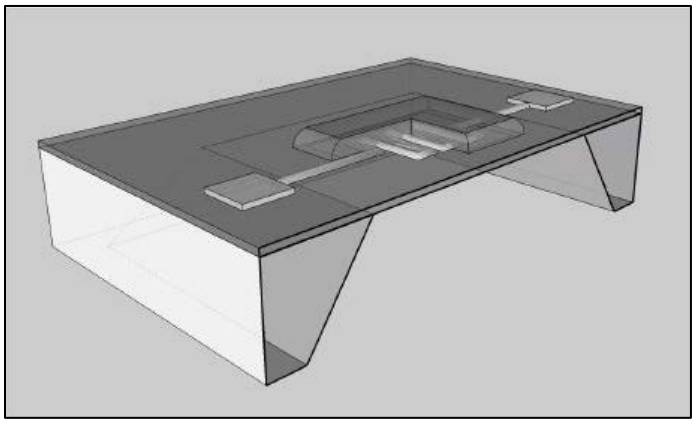

Figure 21: Commercial MEMS pellistor manufactured by SGX (e2v) **[9]**

7. References

[1] J. Janata, Principles of Chemical Sensors, New York: Springer Science & Business Media, 2010.

[2] E. Hunt, D. Reid, D. Space and F. Tilton, "Commercial Airliner Environmental Control System," in *Aerospace Medical Association Annual Meeting*, Anaheim, California, 1995.

[3] J. D. Spengler and D. G. Wilson, "Air Quality in Aircraft," *Proceedings of the Institution of Mechanical Engineers, Part E: Journal of Process Mechanical Engineering*, vol. 217, pp. 323-335, 2003.

[4] "Breathing at High Altitude: The Air Supply of Aircraft Cabins," Lufthansa Technik, [Online]. Available: http://www.lufthansa-technik.com/cabin-air-circulation. [Accessed 29 March 2015].

[5] A. R. Baker, "Improvements in or relating to Electrically Heatable Filaments". Great Britain Patent 892,530, 28 March 1962.

[6] T. Hubert, L. Boon-Brett, G. Black and U. Banach, "Hydrogen Sensors - A Review," *Sensors and Actuators B*, vol. 157, pp. 329-352, 2011.

[7] J. Firth, A. Jones and T. Jones, "The Principles of Detection of Flammable Atmospheres by Catalytic Devices," *Combustion and Flame*, vol. 21, pp. 303-311, 1973.

[8] N. H. Cook and E. Rabinowicz, Physical Measurement and Analysis, Reading, Massachusetts: Addison-Wesley Publishing Company, Inc., 1963.

[9] S. Trautweiler, N. Moser, H. Delprat, S. Lepoutre, C. Alepee, T. Brown and K. Brown, "Disruptive MEMS Technology Replaces Conventional Bead Pellistor Device," in *The 14th International Meeting on Chemical Sensors*, Nuremberg, Germany, 2012.

[10] A. Sussell, M. Singal and P. J. Lerner, "HETA 90-226-2281," ALASKA AIRLINES, SEATTLE, 1993.

[11] D. Basmadjian, Mass Transfer: Principles and Applications, Boca Raton: CRC Press LLC, 2004.

[12] R. W. Fahien, Fundamentals of Transport Phenomena, New York: McGraw-Hill Book

Company, 1983.

[13] R. B. Bird, W. E. Stewart and E. N. Lightfoot, Transport Phenomena, New Dehli: Wiley India, 2008.

[14] Y. A. Cengel, R. H. Turner and J. M. Cimbala, Fundamentals of Thermal-Fluid Sciences, New York: McGraw-Hill Companies, Inc., 2008.

[15] "VQ10 Combustible Gas Detector Elements," SGX Sensortech (formerly e2v), 2008.

[16] "Technical Specification: CH-A3 Combustible Gas Pellistor," Alphasense Ltd., 2012.

[17] A. L. Buck, "Steady State and Transient Response Characteristics of Commercial Carbon Monoxide Sensors," Auburn, AL, 2014.

[18] K. Ogata, System Dynamics, Upper Saddle River, NJ: Prentice Hall, 1998.

[19] T. R. Marrero and E. A. Mason, "Gaseous Diffusion Coefficients," *J. Phys. Chem. Ref. Data*, vol. 1, no. 1, pp. 3-118, 1972.

[20] H. Wong, Handbook of Essential Formulea and Data on Heat Transfer for Engineers, London: Longman, 1977.

[21] M. K. Antoniou, E. K. Diamanti, A. Enotiadis, A. Policicchio, K. Dimos, F. Ciuchi, E. Maccallini, D. Gournis and R. G. Agostino, "Methane storage in zeolite-like carbon materials," *Microporous and Mesoporous Materials*, vol. 188, pp. 16-22, 2014.

Appendix I

Catalyst Determination

The catalyst used on the surface of the SGX VQ10SB detecting pelliment was determined to be thoria by Energy Dispersive Spectroscopy analysis. The aluminum present in Figure A1 is from the alumina support.

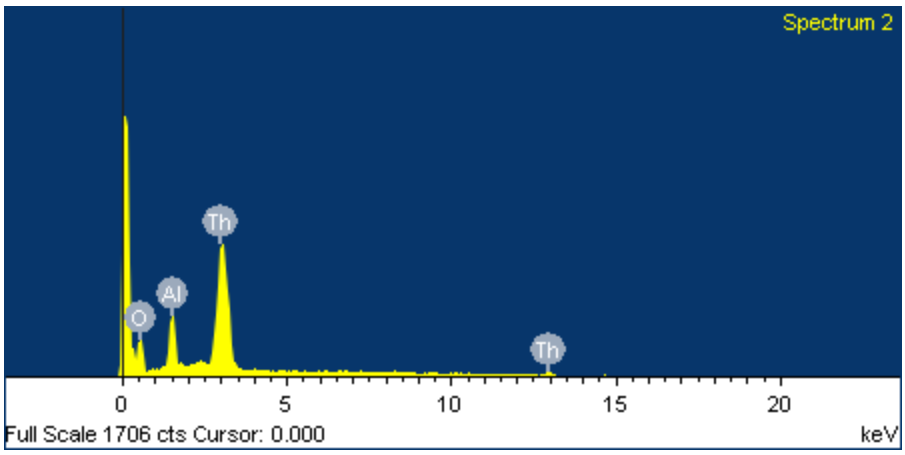

Figure A1: EDS spectra of a SGX detecting pelliment surface

Appendix II

Supplemental Methane Calibrations

The following are supplemental calibrations obtained from steady state testing of the SGX and Alphasense sensors with methane. In Figure A2 the designations “A” and “B” denote the user made circuit board used and the subsequent numerical value denotes specific sensors. In the Case of SGX A2 two separate calibrations were conducted and designated with “a” and “b.” The same designation system was implemented for the Alphasense sensors as seen in Figure A3.

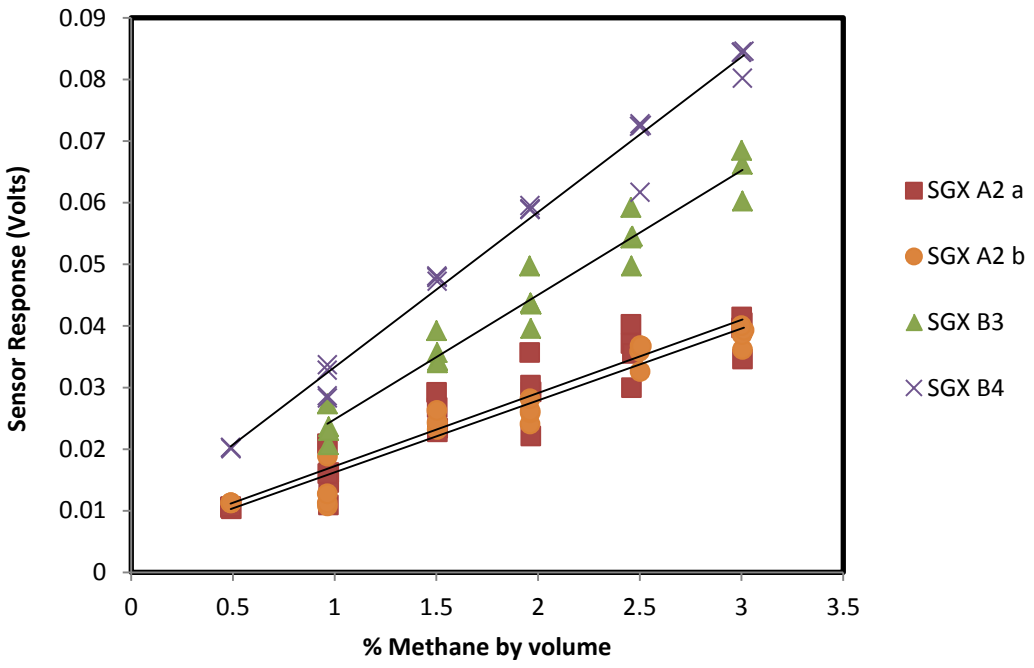

Figure A2: SGX VQ10SB methane calibrations

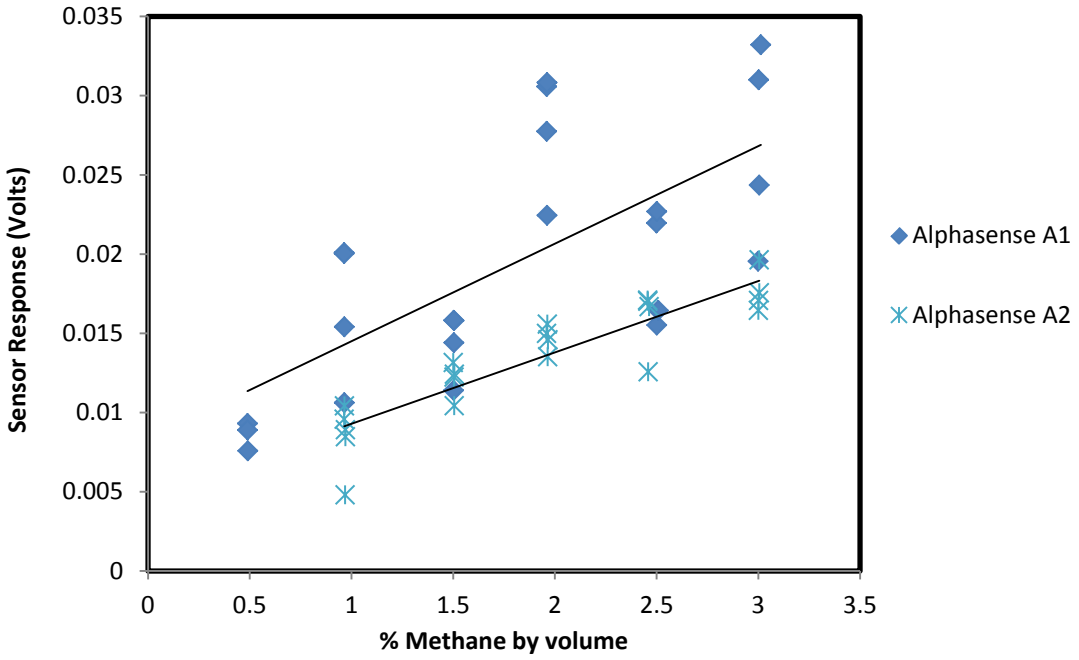

Figure A3: Alphasense CH-A3 methane calibrations

Appendix III

Resistance of Platinum Support for Hotplate Experiments

As discussed in section 4.3.1, the hotplate experimental setup caused the Platinum wire support that the bead is suspended from to reach the same temperature as the bead. Under normal sensor operations, there would be a temperature difference between the bead and the platinum wire outside of the bead. The resistance as a function of temperature was calculated and subtracted from the resistance measurements obtained during hotplate testing. Equations A1 and A2 were used to determine the platinum wire's resistance Where ρ is the resistivity of platinum at a given temperature ($\Omega\, m$), ρ_o is the resistivity of platinum at a reference temperature ($\Omega\, m$), α is the temperature coefficient of platinum (K^{-1}), T is the given temperature (K), T_o is the reference temperature (K), R is the resistance of the platinum wire (Ω), L is the length of the wire (m), and A_{cs} is the cross sectional area of the wire (m^2).

$$\rho = \rho_{o\,[1+\,\alpha(T-T_o)]} \qquad \text{A1}$$

$$R = \frac{L\,\rho}{A_{cs}} \qquad \text{A2}$$